

Module Test Studies for the CMS Tracker Upgrade

Stephanie Yuen
Tufts University, Medford, MA USA

September 9, 2010

DESY Summer Student Programme 2010



Abstract

The sLHC luminosity upgrade aims to obtain better statistics for events recorded by detectors. As part of this upgrade, one of the goals for the CMS inner tracking detector upgrade is to increase granularity while reducing the material budget. The test setup facilities achieved in this project will allow for measurements of prototype modules for the future tracker outer barrel. Optimization of the test setup was achieved by comparing experimental thermal conductivity values to known literature.

Contents

1	Introduction	2
2	Experimental apparatus	3
3	Intercalibration of Pt-100 sensors	4
4	Thermal conductivity	8
4.1	Data	8
4.2	Analysis	9
5	Conclusion and Outlook	11
6	Bibliography	11
7	Acknowledgements	12

1 Introduction

Studies are underway for the proposed sLHC (super Large Hadron Collider) upgrade of luminosity. Higher luminosity will allow for more interactions per bunch crossing and a greater number of particles, i.e., the number of particles per unit area per unit time multiplied by the opacity of the target. Currently, the LHC is capable of proton-proton collisions at a center of mass energy of 14 TeV. At full luminosity of $10^{34} \text{ cm}^{-2} \text{ s}^{-1}$, there are 2,808 bunches per beam, with 1.15×10^{11} protons per bunch. The sLHC expects to have a luminosity increase by a factor of 10 with the principle aim of obtaining better statistics for events.

However, the upgrade also entails radiation damage and over-occupancy of detectors. The plan for the CMS (Compact Muon Solenoid) detector, which exploits the different properties of the particles it captures to measure their energy and momentum, consists of a tracker upgrade. Because of the nature of their current operation, the silicon strip detectors of CMS will experience diminishing returns as the detectors and electronics suffer from radiation damage. With the sLHC upgrade, the plans for CMS are to increase granularity to compensate for over occupancy and to design modules for cooling efficiency while minimizing the material budget.

The DESY CMS Tracker Upgrade group is involved in investigations of cooling efficiency and low temperature operation of sensors, in order to preserve the lifetime of sensors as a higher flux of particles pass through and suffer less damage due to radiation. Modules should be designed to drag resultant heat out without compromising the material budget.

During the DESY Summer Student Programme, I worked on the test facility for measuring and optimizing thermal gradients across interfaces. I combined finite element simulations of Gmsh and GetDP and the module test facilities. Gmsh generates 3-D finite elements for getDP, a finite element solver for simulations of temperature and heat flux for test structures. To achieve these goals, I gained experience with temperature calibration and performing measurements on understood test structures. This will allow for future measurements of actual module research and development. Thermal stability analyses will lead to new module designs for the future tracker outer barrel.

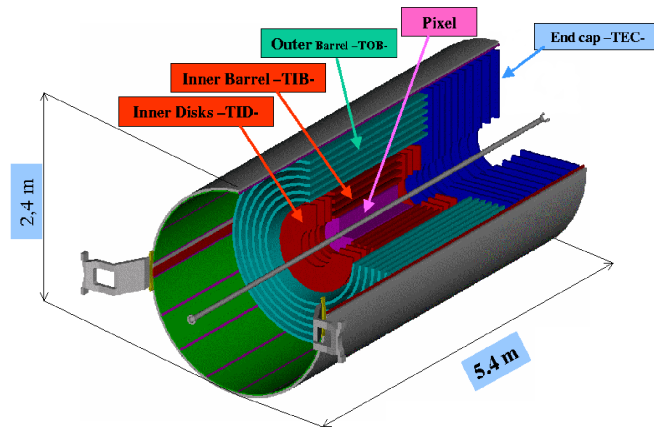


Figure 1: CMS Detector

2 Experimental apparatus

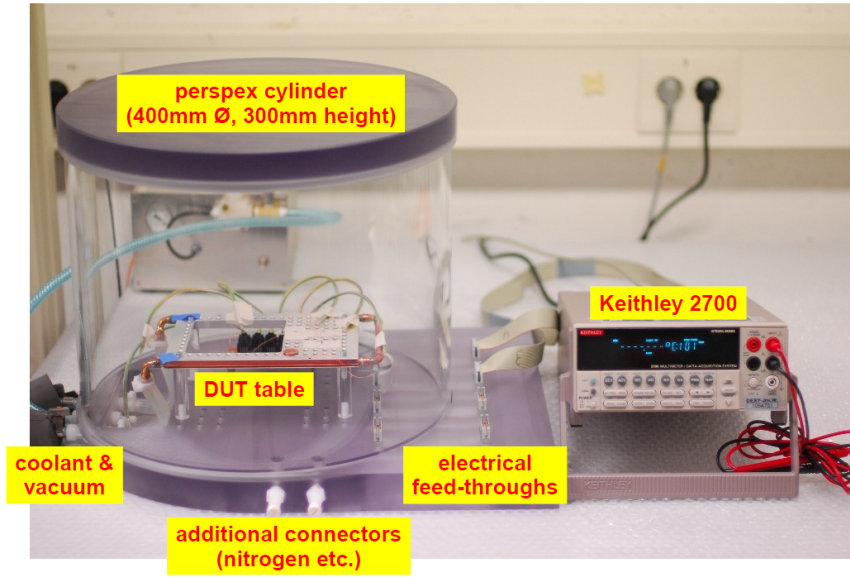


Figure 2: Experimental setup

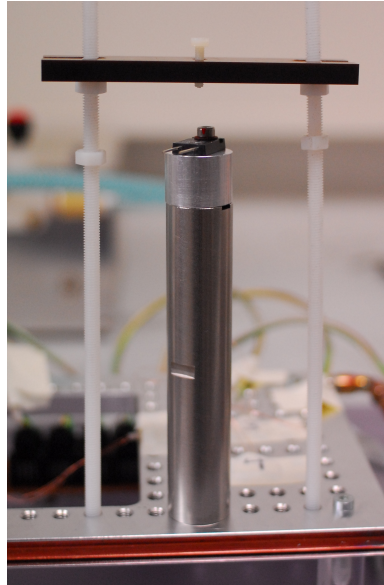


Figure 3: Rod with heat spreader and resistor

Measurements of the thermal conductivity of test structures were performed using the setup pictured in Figures 2 and 3. To minimize systematic effects due to convection, a Plexiglass vacuum cylinder of cross sectional area of 400 mm and height of 300 mm was evacuated to maintain a stable pressure of about -0.95 bar. Silicon oil from a conventional chiller (Julabo FP50-MC with 160 W cooling power) circulated around the DUT table in a copper cooling loop.

Throughout the setup, a paste with high thermal conductivity was applied to optimize heat transfer between thermal interfaces between two different materials and between materials and sensors. Pt-100 sensors with electrical feedthroughs to a Keithley 2700 measured the temperature at strategic points in the setup. These sensors were attached using paste with high thermal conductivity.

An aluminum heat spreader with the same cross sectional area as the material probes transferred heat from various resistors to the top of the material probes. The goal was to achieve uniform heat distribution on the top of the rod.

For measurements with the steel rod, which are shown in Figure 10, $\frac{dQ}{dt} = 0.20376 \text{ W}$ produced by a total resistivity of 2.264Ω with two wires soldered to a resistor and a current of 0.300 A. For measurements with the aluminum rod, which are shown in Figure 11, $\frac{dQ}{dt} = 6.124 \text{ W}$ produced by a total resistivity of 98.779Ω with two wires soldered onto a resistor and a current of 0.249 A.

The value for the power current was chosen based on the limit of 300 mA for the vacuum feed through a vacuum feedthrough and the desire to minimize system effects in measurement by achieving a large temperature difference along the rod. In principle, to achieve a temperature difference of about 10 K on the rod, based on a literature value of $k = 15 \text{ W/m/K}$ for stainless steel,

$$\begin{aligned} \frac{dQ}{dt} = RI^2 &= k_{\text{Stainlesssteel}} A_{\text{rod}} \frac{\Delta T}{\Delta x} \\ &= (15 \text{ W/m/K})(0.000320 \text{ m}^2) \left(\frac{10 \text{ K}}{0.098 \text{ m}} \right) \\ I &= 0.465 \text{ A} \end{aligned}$$

Because the vacuum feedthrough has a limit of 300 mA, the resistor for the Stainless steel setup was replaced with one of larger resistance. Additionally, the stainless steel material probe was replaced with an Aluminum one whose thermal conductivity of $k = 250 \text{ W/m/K}$ is more well verified.

$$\begin{aligned} \frac{dQ}{dt} = RI^2 &= k_{\text{Al}} A_{\text{rod}} \frac{\Delta T}{\Delta x} \\ &= (250 \text{ W/m/K})(0.000320 \text{ m}^2) \left(\frac{10 \text{ K}}{0.098 \text{ m}} \right) \\ I &= 0.287 \text{ A} \end{aligned}$$

3 Intercalibration of Pt-100 sensors

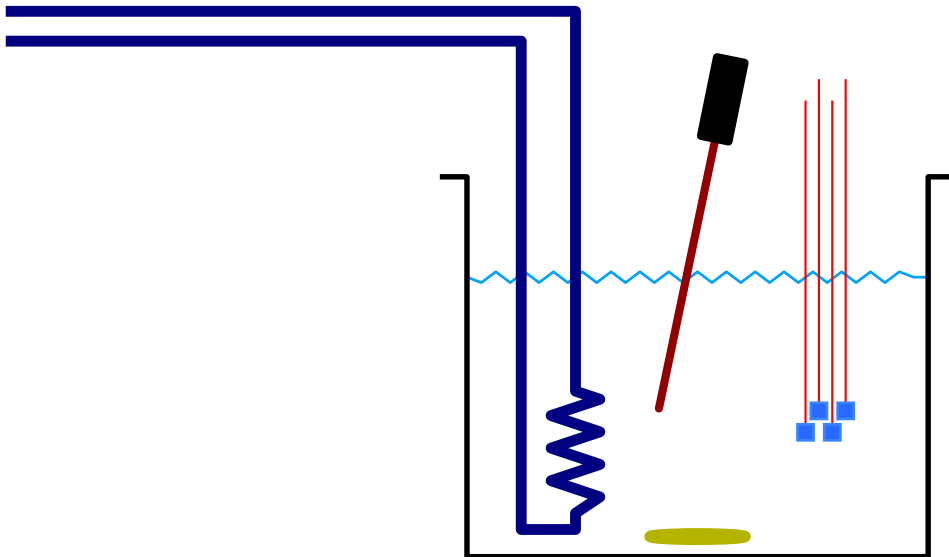


Figure 4: Calibration setup

In order to analyze the thermal conductivity of test structures, the Pt-100 sensor needed to be intercalibrated first, using the calibration setup shown in Figure 4. The Pt-100 sensors each had offsets, which are the difference in temperature measured between each Pt-100 sensor and the temperature probe.

To create a stable environment for measuring temperature and then correlating them to the reference temperature, the sensors and reference probe were placed in a stirred bath of ethanol, inside an insulated cube. The ethanol bath temperature was controlled by silicon oil coolant from a conventional chiller (Julabo FP50-MC with 160 W cooling power). The operation parameters for Julabo FP50-MC were tuned to minimize fluctuations in the silicon oil bath.

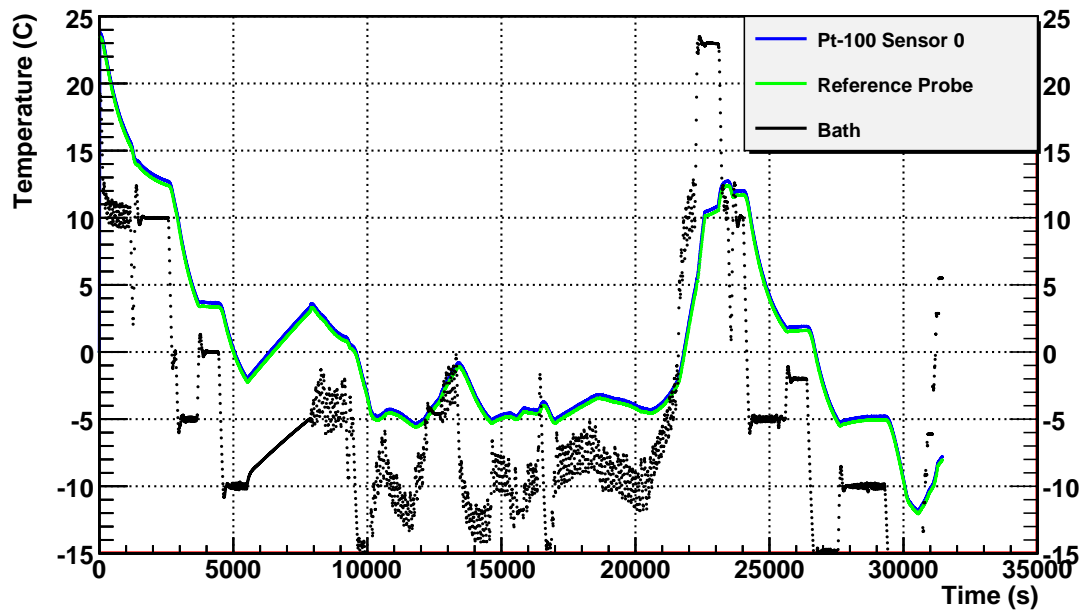


Figure 5: Temperature measurement of the ethanol bath taken by Reference Probe and the 10 Pt-100 Sensors (only sensor 0 shown here) as a function of time. Fluctuations in bath temperature are a result of attempts to fine-tune the PID parameters for stable temperature. (August 5, 2010, 110340)

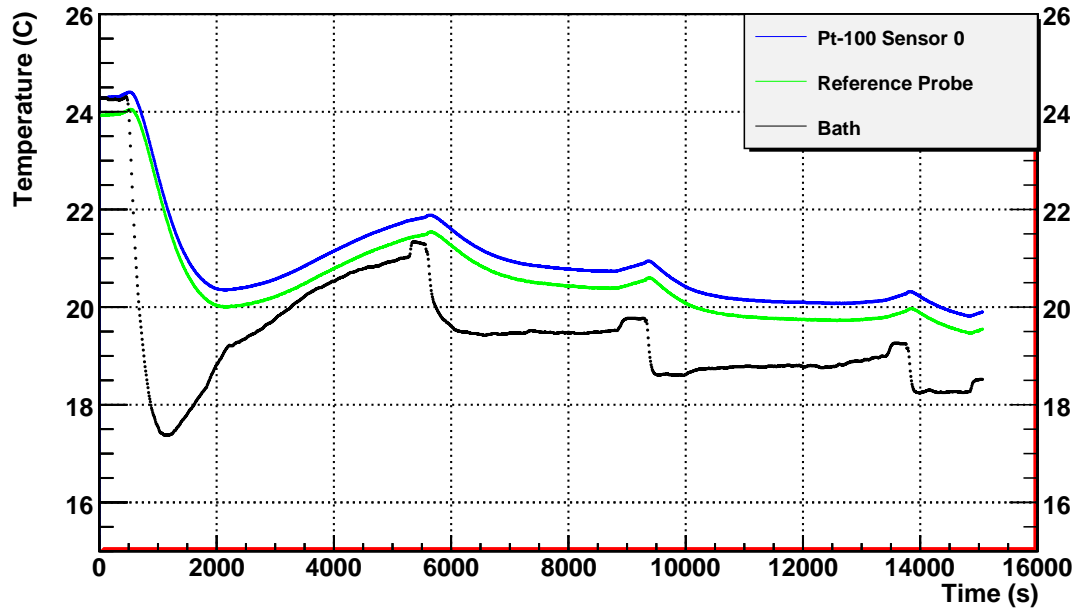


Figure 6: Temperature measurement of the ethanol bath taken by Reference Probe and the 10 Pt-100 Sensors (only sensor 0 shown here) as a function of time. Stable temperatures were maintained for longer periods of time. (August 9, 2010, 092114)

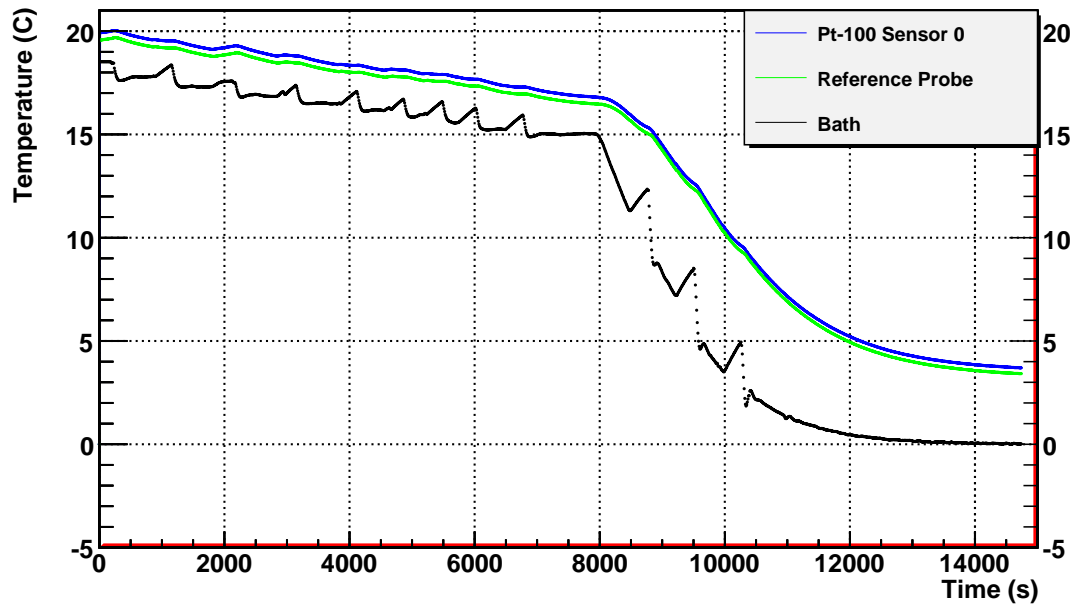


Figure 7: Temperature measurement of the ethanol bath taken by Reference Probe and the 10 Pt-100 Sensors (only sensor 0 shown here) as a function of time. The peaks and troughs in the bath temperature occurred due to experimentation with PID parameters. (August 9, 2010, 133252)

In figures 5, 6, and 7, the aim was to take measurements at different levels of stable temperature. Data were taken for a range from -20°C to 30°C to obtain calibration constants from the y -intercept in a linear fit. Measuring over a wide range allows for checks of nonlinearities in comparing data taken by the temperature probe and each Pt-100 sensor.

Long time delays in the readout between the reference probe and the Pt-100 sensors occurred for large slopes, $\frac{\Delta T}{\Delta t}$. This was evident in mismatch of the peaks and troughs seen in the data. Therefore, a slope restriction was applied in calibration calculations. T_{ref} is ignored in offset calculation if

$$\left| \frac{\Delta T_{ref}}{\Delta t} \right| > 0.001 \quad (1)$$

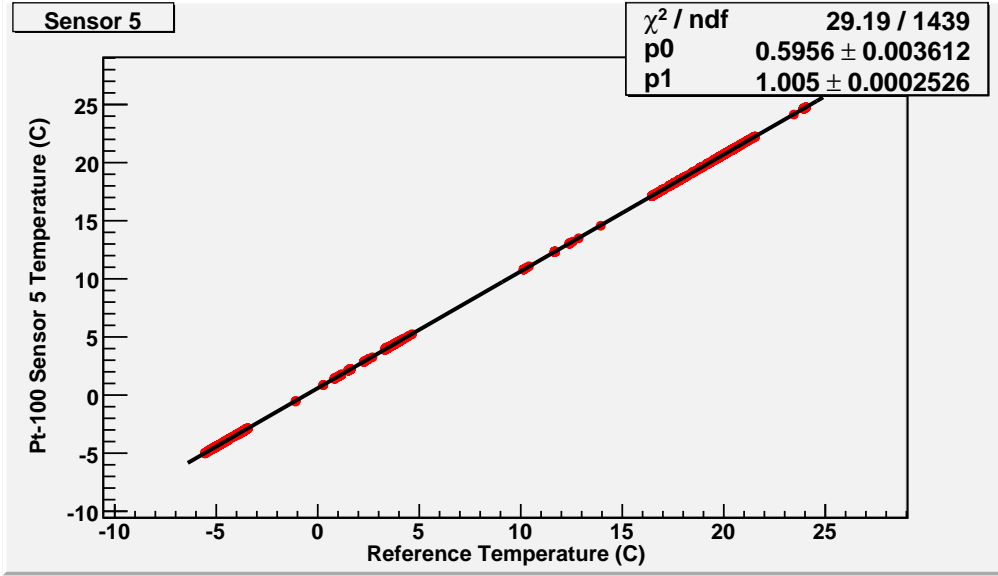


Figure 8: Example of calibration fit for Pt-100 Sensor 4

Figure 8 is a an example of a plot of a Pt-100 Sensor Temperatureas a function of Reference Probe Temperature. The goal is to match the temperatures and find the y -intercept, or $p0$, when Pt-100 Sensor temperature is 0 using a straight line fit. The graph takes in three different data measurements (see Figures 5, 6, 7), excluding all points where $\left| \frac{\Delta T_{ref}}{\Delta t} \right| > 0.001$. As expected, the slope, $p1$, is close to 1. The y -intercepts for each Pt-100 Sensor vs. Reference Temp straight line fit were entered into temperature measurements taken for thermal conductivity.

4 Thermal conductivity

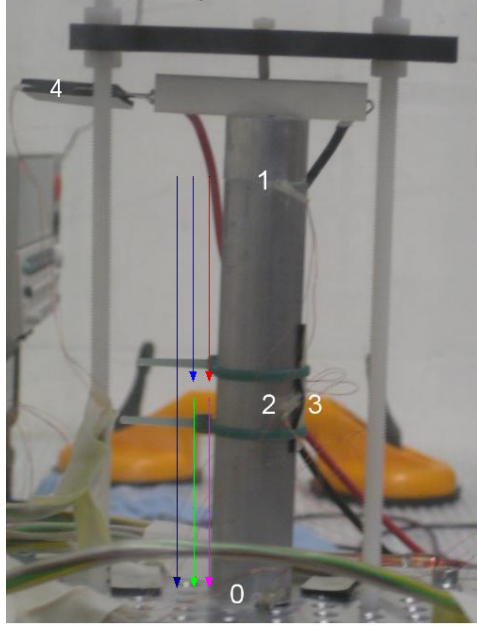


Figure 9: Color coding for temperature gradient measured with Sensors 0-5. Sensor 4 is near the resistor, and Sensor 5 (not shown) is on the wire

Thermal conductivity, k , is a measurement of the relation of a material's rate of heat lost per unit area to the rate of temperature change.

$$\frac{dQ}{dt} = kA \frac{\Delta T}{\Delta x} \quad (2)$$

Measuring the thermal conductivity of test structures against known literature provides insight into optimization of the module test facilities.

4.1 Data

Data were taken using the setup shown in Figures 2 and 3. The setup in Figure 9 shows the placement chosen for the sensors to measure temperature gradients. Sensor 0 is located in the 1 mm high notch between the rod and the table, Sensor 1 is in the notch between the rod and the heat spreader, Sensors 2 and 3 are in the notch in the middle of the rod, Sensor 4 (not shown) is near the resistor, and Sensor 5 (not shown) is 20 cm from the Sensor 4, along the wire. This allowed for observation of temperature differences on the rod and along the wire. In principle, the difference in temperature between Sensors 4 and 5 can provide insight into the power lost from the resistor and correct for $\frac{dQ}{dt}$ used in thermal conductivity calculations.

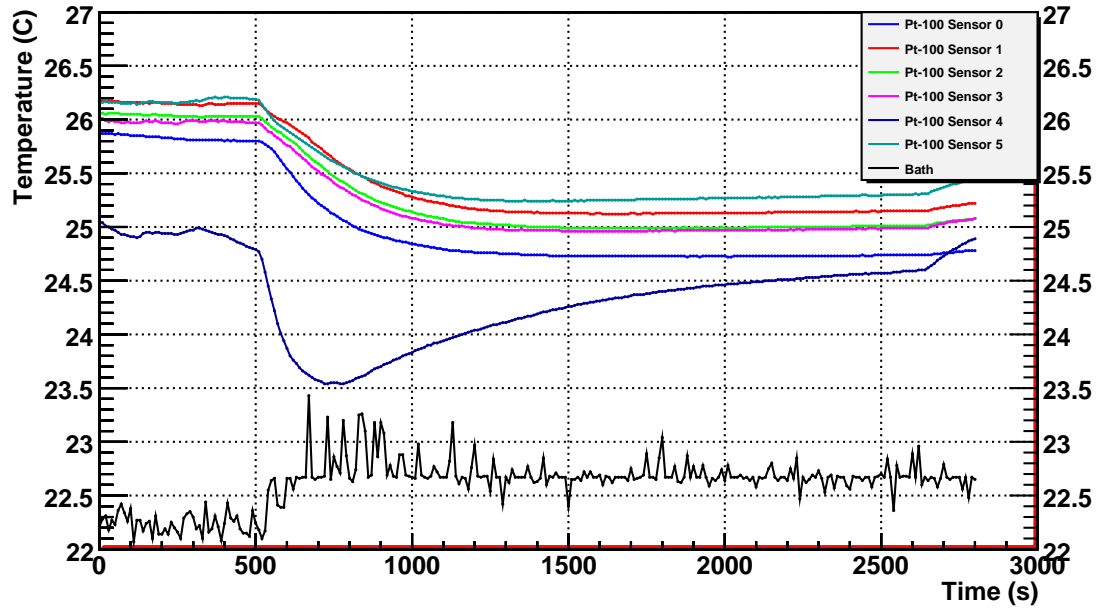


Figure 10: Temperature measured by Pt-100 Sensors 0-5 and Bath as a function of time (August 19, 2010, 153026)

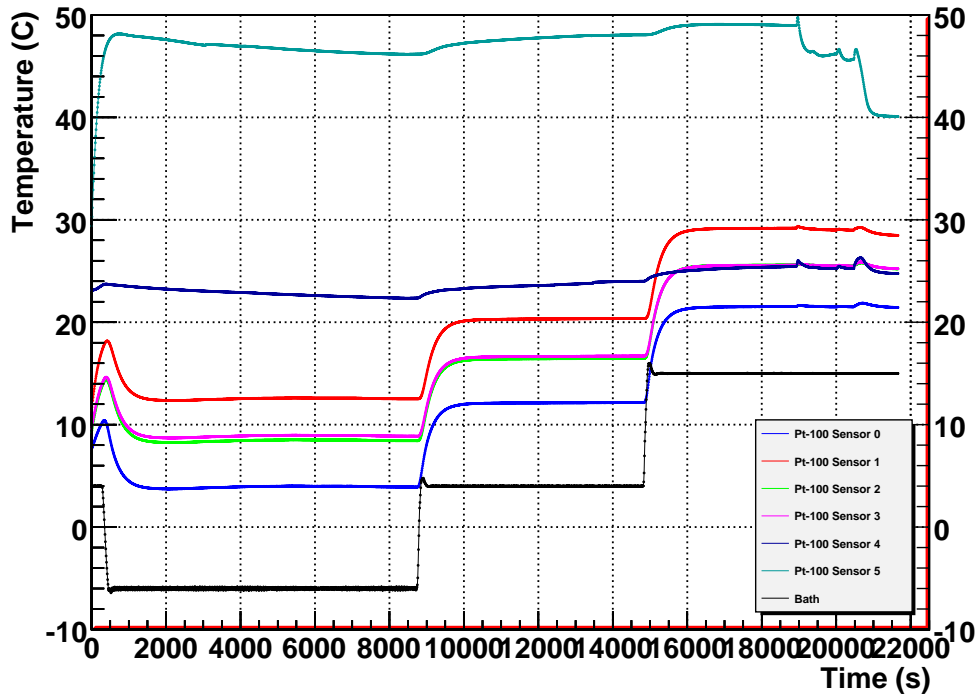


Figure 11: Temperature measured by Pt-100 Sensors 0-5 and Bath as a function of time (August 26, 2010, 110837)

4.2 Analysis

For thermal conductivity calculated in Figure 12, the power is $\frac{dQ}{dt} = 0.20376 \text{ W}$, the cross sectional area of the rod is $A_{rod} = 3.14(0.0101 \text{ m})^2$, and the total height of the rod is $\Delta x_{1-0} =$

0.098 m.

For the power lost, the thermal conductivity of the copper wire is $k_{Cu}=395$ W/m/K, the cross sectional area of the wire is $A_{wire} = 10^{-6} \text{ m}^2$, $\Delta x = 0.20$ m.

From Figure 10 for the stainless steel rod, $\Delta T_{5-4} = 25.25 - 24.5 = 0.75 \text{ K}$

$$\begin{aligned} \frac{dQ}{dt} &= k_{Cu} A_{wire} \frac{\Delta T}{\Delta x} \\ &= (395 \text{ W/m/K})(10^{-6} \text{ m}^2) \left(\frac{0.75 \text{ K}}{0.40 \text{ m}} \right) \\ &= 0.00740 \text{ W} \end{aligned}$$

The power generated by the resistor and current from the Keithley 2700 power source is 0.20376 W. The percentage of the power recovered is

$$\left(\frac{0.20376 \text{ W} - 0.00740 \text{ W}}{0.20376 \text{ W}} \right) (100) = 96.37\%$$

From Figure 11 for the aluminum rod, $\Delta T_{5-4} = 47 - 23 = 24 \text{ K}$.

$$\begin{aligned} \frac{dQ}{dt} &= k_{Cu} A_{wire} \frac{\Delta T}{\Delta x} \\ &= (395 \text{ W/m/K})(10^{-6} \text{ m}^2) \left(\frac{24 \text{ K}}{0.40 \text{ m}} \right) \\ &= 0.24 \text{ W} \end{aligned}$$

The power generated by the resistor and current from the Keithley 2700 power source is 6.124 W. The percentage of the power recovered is

$$\left(\frac{6.124 \text{ W} - 0.24 \text{ W}}{6.124 \text{ W}} \right) (100) = 96.08\%$$

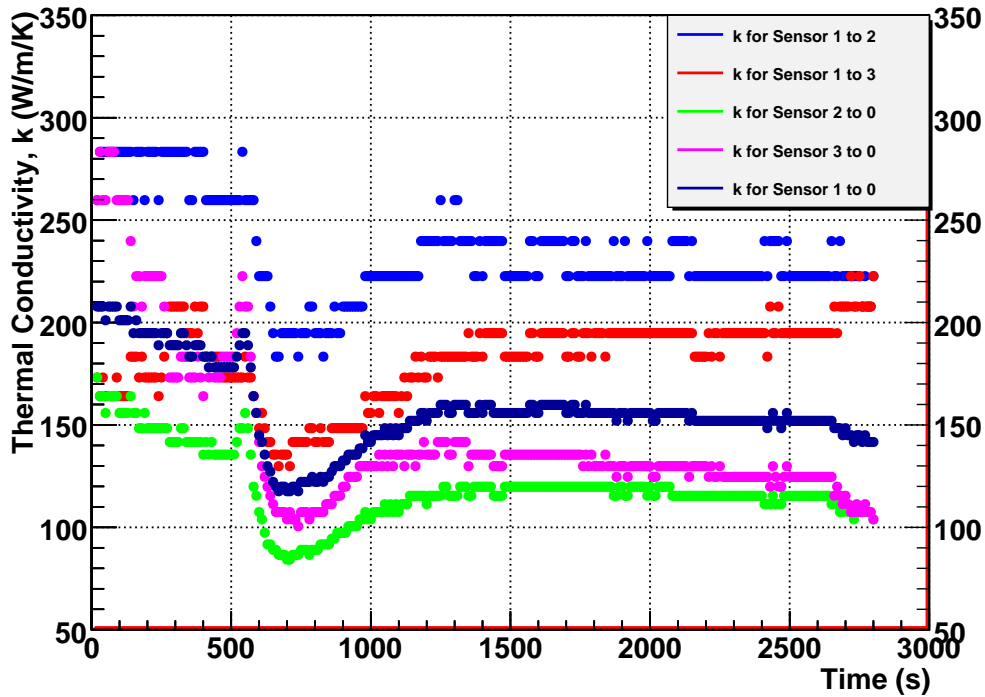


Figure 12: Thermal conductivity of steel rod for different sensor positions and different bath temperatures as a function of time (August 19, 2010, 153026)

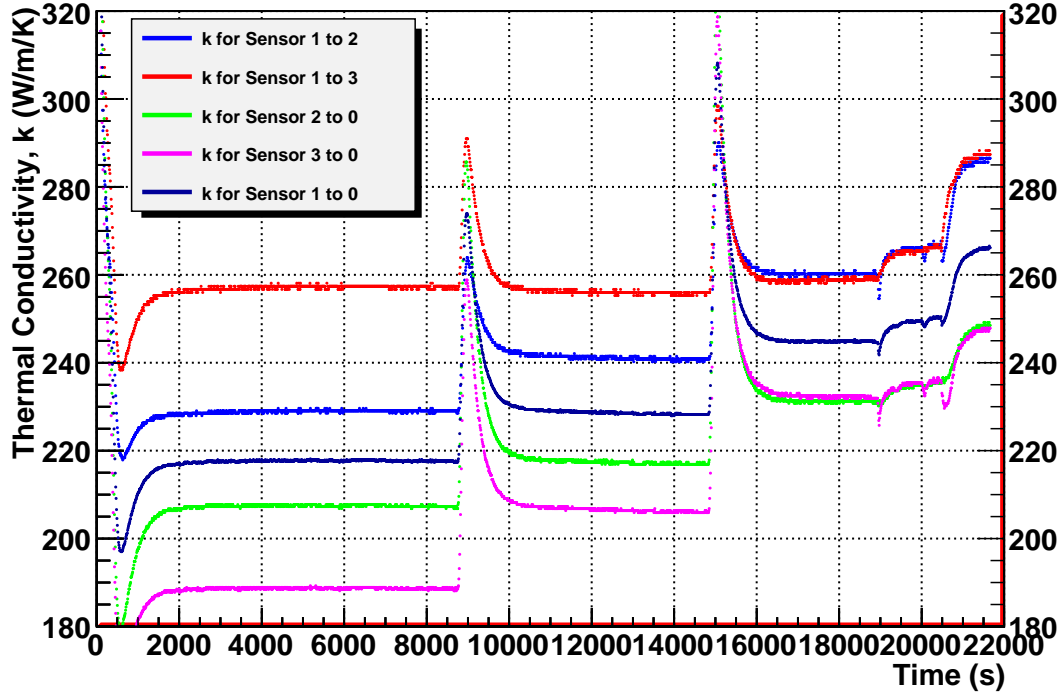


Figure 13: Thermal conductivity of steel rod for different Δx and different bath temperatures as a function of time (August 26, 2010, 110837)

In Figures 12 and 13, thermal conductivity should be indicative of the sensors used. In principle, since sensors 2 and 3 are at the same height along the material probe, k_{1-2} and k_{1-3} should be equal, as should k_{2-0} and k_{3-0} . The experimental calculations, however, do not match these predictions and show great differences. Also, the temperature differences from Sensor 1 to Sensors 2, 3 and than those from Sensors 2, 3 to Sensor 0. Additionally, the thermal conductivity measured seems to depend greatly on the temperature at which the bath operated. This spread in thermal conductivity should not be so big.

5 Conclusion and Outlook

To improve the module test module setup and confirm thermal conductivity values achieved by the setup that can be verified by literature, systematic errors should be minimized. Improvements should be made on evacuation of the vacuum to minimize convection, insulation of the material probe, attachment of sensors, use of conductivity paste for thermal interfaces between materials, and estimation of $\frac{dQ}{dt}$ factoring in the heat lost over the cable. Though Sensors 2 and 3 are located right next to each other in the middle of the cylinder (both 0.049 m from bottom), they show significant difference in thermal conductivity.

Investigations of mechanical deformation due to thermal stress

6 Bibliography

Olzem, J., Eckerlin, G., Hansen, J., Muhl, C., Mussgiller, A. (2010, May) *Status and plans for module test facilities at DESY Hamburg*. CEC Zeuthen.

Mussgiller, A., Eckerlin, G., Hansen, J., Muhl, C., Olzem, j. (2010, May) *Module design and finite element calculations*. CEC Zeuthen.

7 Acknowledgements

I would like to acknowledge my supervisors, Andreas Mussgiller and Jan Olzem, for their guidance with this project. I would also like to thank my colleague, Francesco Costanza, for his help with the project and the friendly atmosphere he created. Last but not least, I would like to acknowledge the DESY Summer Student Programme 2010, especially the coordinators, Joachim Meyer and Andrea Schraeder.